Jahn-Teller Interactions in the Dissociative Recombination of H_3^+

Ch. Jungen[1,*] and S. T. Pratt[2]

[1]*Laboratoire Aimé Cotton du CNRS, Bâtiment 505, Université de Paris-Sud F91405 Orsay, France*
[2]*Argonne National Laboratory, Argonne, Illinois 60439, USA*
(Received 2 October 2008; published 16 January 2009)

A simple analytical approach is presented to describe the dissociative recombination (DR) of an electron with H_3^+ and its isotopomers. The principal assumption is that resonant capture mediated by the Jahn-Teller interaction dominates the cross section. The only input required comes from spectroscopic data on the $3pE'$ Rydberg state of H_3 and the ν_2 vibrational frequencies of H_3^+ and its isotopomers. The approach provides an independent prediction of the low-energy DR cross sections and rates, and is in good agreement with the latest experimental and theoretical determinations.

The central role of H_3^+ in chemical reaction networks in interstellar space has generated considerable interest in its principal loss mechanism, dissociative recombination (DR) with electrons [1–4], corresponding to the process $H_3^+ + e^- \rightarrow H_2 + H$ or $H + H + H$. From a fundamental perspective, this is the simplest polyatomic system for DR, and the process has attracted considerable experimental and theoretical attention. After many years of discrepancies and controversy, the data from numerous experiments now appear to be converging [4,5], and the theoretical results [6–9] are converging to the experimental results. Perhaps the most notable aspect of the DR of H_3^+ to come from the theory has been the discovery that the Jahn-Teller (JT) interaction is a key factor in the recombination process [6–9]. In particular, previous calculations of the DR rate were too low by orders of magnitude, but with the inclusion of the JT interaction [6–9], the agreement between experiment and theory is dramatically improved.

The theoretical treatment of H_3^+ DR by Kokoouline and Greene required the application of some of the most advanced techniques of molecular physics, and their calculations involved thousands of reaction channels [9]. More generally, nonadiabatic effects, that is, processes involving the nonseparability of electronic and nuclear motion, are notoriously difficult to treat because they require knowledge of the electronic wave functions as well as the electronic energies. There are, however, several classic examples of nonadiabatic effects that can be treated analytically, including the Hill and van Vleck treatment of spin uncoupling in doublet Π states of diatomic molecules, the Renner-Teller effect in linear molecules, and the JT effect in weakly distorted molecules [10]. Because the JT effect is a crucial feature of the DR of H_3^+, it is tempting to see whether the existing analytic results can be adapted to this process.

H_3^+ is also the simplest member in a class of protonated closed-shell systems with considerable astrochemical interest. While such species tend to be quite stable, capture of an electron leads to the production of a Rydberg molecule [11], which tend to be unstable with respect to dissociation. This general situation supported an approximation in the initial work [6] on H_3, in which it was assumed that electron capture was the rate limiting step in the DR of H_3^+, and that all successful capture processes led to dissociation. While later work included the dissociation process explicitly [8,9], it is not thought that this has a substantial effect on the theoretical cross section.

In this Letter, we propose an analytic treatment of the DR process in H_3^+. This treatment is based on the above approximation and uses spectroscopically determined data to evaluate the capture cross section. To do this, we use the approach of multichannel quantum defect theory (MQDT), in which a unified treatment of bound and continuum states allows the use of data on the bound (with respect to ionization) states of H_3 to determine the widths of autoionizing resonances above the ionization threshold.

Let us review some basic features of the JT theory for a D_{3h} molecule such as H_3 [12]. Let $Q_\pm = \rho e^{\pm i\phi}$ be the two components of the degenerate ν_2 vibrational mode, with ρ the nuclear displacement amplitude and ϕ its phase. If the three identical nuclei are rotated clockwise by $2\pi/3$ (C_3 symmetry operation, called C in the following) the phase of the nuclear displacements increases according to $\phi \rightarrow \phi + \frac{2\pi}{3}$, with the result that $CQ_+ = \omega Q_+$ and $CQ_- = \omega^* Q_-$ where $\omega = e^{2i\pi/3}$ (see Fig. 1) Let now ψ_+ and ψ_- be two electronic wave functions representing the two degenerate p orbitals lying in the molecular plane forming a pe' Rydberg state. Their angular dependences are $e^{+i\Lambda\phi}$ and $e^{-i\Lambda\phi}$ with $\Lambda = 1$. It is easy to see (cf. Fig. 1) that when the operation C is applied to the nuclei with the electronic orbitals kept fixed in space, the phase of the electronic wave functions is *decreased* by $\frac{2\pi}{3}$ so that we have $C\psi_+ = \omega^* \psi_+$ and $C\psi_- = \omega \psi_-$.

In JT theory [12] the electronic Hamiltonian $H_e(Q_+, Q_-)$ is expanded near the symmetric configuration in terms of a power series involving Q_+ and Q_-. The electronic matrix arising in this expansion involves matrix elements such as
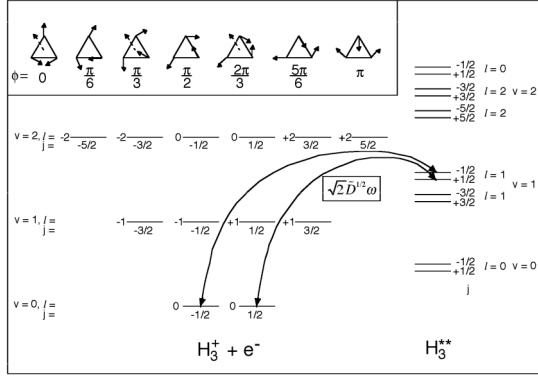
FIG. 1.   Schematic diagram of the levels involved in the DR of H_3^+ with an electron. With the linear Jahn-Teller (JT) effect, only $\Delta v = \pm 1$ processes are allowed, and the coupling between the $v = 0$ and 1 levels is shown with the double arrows. The arrows pointing to the right (left) indicate electron capture (JT vibrational autoionization), respectively. The scaled matrix element coupling the continuum and Rydberg states is also indicated. Inset: nuclear displacements corresponding to the degenerate JT vibrational mode. The dotted arrow indicates the phase of the electronic factor $e^{i\Lambda\phi}$.

$$\int \psi_+^* H_e(Q_+, Q_-)\psi_- dq = V_0 + \sum_i V_i Q_i$$
$$+ \frac{1}{2}\sum_{ij} V_{ij} Q_i Q_j + \ldots, \quad (1a)$$

$$\int \psi_+^* H_e(Q_+, Q_-)\psi_+ dq = W_0 + \sum_i W_i Q_i$$
$$+ \frac{1}{2}\sum_{ij} W_{ij} Q_i Q_j + \ldots, \quad (1b)$$

where i and j take the values $+$ and $-$. Since $H_e(Q_+, Q_-)$ is invariant under the operation C, the integral of, e.g., Eq. (1a) transforms like the product $\psi_+^* \psi_-$, i.e., as $\omega^2 = \omega^* = e^{-2i\pi/3}$. Therefore on the right-hand side of Eq. (1a) the real coefficients multiplying Q_- and Q_+^2 will be non-vanishing whereas the other terms are zero.

Based on this type of argument the matrix of $H_e(Q_+, Q_-)$ is established [12] to have the form

$$\mathbf{H}(\rho, \phi) = \begin{pmatrix} W_0 + \frac{1}{2}k\rho^2 & f\rho e^{-i\phi} + g\rho^2 e^{2i\phi} \\ f\rho e^{i\phi} + g\rho^2 e^{-2i\phi} & W_0 + \frac{1}{2}k\rho^2 \end{pmatrix},$$
(2)

where we have made the substitutions $V_- \rightarrow f$ and $W_{+-} \rightarrow k$, and so forth. Diagonalization of the matrix Eq. (2) yields the real electronic Born-Oppenheimer potential surfaces $U_{1,2}(\rho, \phi)$ as well as the real electronic Born-Oppenheimer eigenfunction angular factors $\psi_{1,2}$. We obtain

$$U_{1,2} = W_0 + \frac{1}{2}k\rho^2 \pm \left[f\rho + \frac{1}{2}g\rho^2 \cos 3\phi \ldots \right], \quad (3)$$

and, for small ρ values where the quadratic off-diagonal

term in Eq. (2) may be neglected,

$$\psi_1 = (2)^{-1/2}[\psi_+ e^{-i\phi/2} + \psi_- e^{i\phi/2}] \sim \cos(\phi/2), \quad (4a)$$
$$\psi_2 = (2)^{-1/2}[-i\psi_+ e^{-i\phi/2} + i\psi_- e^{i\phi/2}] \sim \sin(\phi/2). \quad (4b)$$

The potential surfaces Eq. (3) exhibit the well-known features of JT distortion [12]: (i) there is a conical intersection at the symmetric position $\rho = 0$, (ii) the linear term lowers the potential minima by the amount $f^2/2k$, and (iii) the quadratic term introduces three minima in the lower potential trough. The eigenfunctions Eq. (4) reveal the effect of Berry's phase [13] as they correspond to an electronic angular momentum $\Lambda = 1/2$ instead of $\Lambda = 1$ and they are *not* eigenfunctions of the symmetry operation C since, in particular, the identity operation $I = C^3$ yields $C^3\psi_{1,2} = -\psi_{1,2}$.

We introduce nuclear motion along the JT coordinates Q_+ and Q_-, retaining only the linear term in Eq. (2). The zero-order level diagram (neglecting the JT term) up to $v = 2$ is shown in Fig. 1. The total angular momentum is composed of the vibrational component, $\pm l$, with l integral, and the electronic component $\pm 1/2$. The sum $j = l \pm 1/2$ is conserved in the linear approximation because there are no ϕ-dependent terms in the potential in this situation, j takes the values indicated in Fig. 1. The vibronic matrix elements then involve integrals over $f\rho$ evaluated with two-dimensional harmonic oscillator functions $|v, l\rangle$. The analytical expressions for these integrals [12] are expressed with the dimensionless JT parameter $D = f^2/2k\omega$ which measures the lowering of the potentials by the linear term in units of the vibrational frequency $\omega = (2\pi)^{-1}[hk/(M_\rho c)]^{1/2}$, where the force constant k is expressed with cm^{-1} as energy units and M_ρ is the relevant mass factor. Using the relation $f[h/(8\pi^2 M_\rho c\omega)]^{1/2} = D^{1/2}\omega$, we obtain the matrix element connecting the levels $v = 0, l = 0, j = \pm 1/2$, and $v = 1, l = \pm 1, j = \pm 1/2$ as

$$f\langle v = 1, l = \pm 1|\rho|v = 0, l = 0\rangle = D^{1/2}\omega\sqrt{2}. \quad (5)$$

We now show that this matrix element, with appropriate values for D and ω, provides a realistic description of the DR of H_3.

We consider only the linear JT effect, and thus are limited to capture processes involving $\Delta v_2 = 1$. The propensity rule for vibrational autoionization [14,15] (the reverse process of electron capture) suggests that this will be the dominant process. Figure 1 shows a schematic diagram of this process, with the matrix element for the coupling between the initial and final states indicated. The quantity $D^{1/2}$ of Eq. (5) has been replaced by the scaled quantity $\tilde{D}^{1/2}$ required in the quantum defect language by dividing by the spacing between adjacent levels, $2\mathcal{R}/n^{*3}$, i.e.,

$$\tilde{D}^{1/2} = \frac{n^{*3}}{2\mathcal{R}} D_{n^*}^{1/2}, \quad (6)$$

where n^* is the effective principal quantum number, $\mathcal{R}$ is

the Rydberg constant, and D_{n^*} is the JT parameter of the Rydberg state n^*. Here we connect to spectroscopic data [16,17] by using the previously determined value of D for the $3pE'$ state of H_3 with $n^* = 2.634$ and $D = 0.0301$. The quantity $D\omega$ is purely electronic and therefore isotope independent, and we use the same value for all four isotopomers. The ω values for the different isotopomers are assumed to be equal to those of the ion, ω^+, which are known from accurate *ab initio* calculations [18,19]. With these ω values, the isotope dependence of D can be determined, and the matrix elements can be obtained. The relevant values are summarized in Table I.

Using the scaled interaction provided above and the golden rule expression, the autoionization width, Γ_a, of a single level with principal quantum number n^* is [15]

$$\Gamma_a = 2\pi \frac{2\mathcal{R}}{n^{*3}} |\sqrt{2}\tilde{D}^{1/2}\omega|^2. \tag{7}$$

With the approximation that electron capture is the determining step, the DR cross section for a single resonance is given by the Breit-Wigner expression

$$\sigma^{\text{res}}(E) = \frac{4\pi}{k^2} \frac{\frac{1}{4}\Gamma_a\Gamma}{(E - E_{\text{res}})^2 + \frac{1}{4}\Gamma^2}, \tag{8}$$

where k is the wave number of the electron and Γ is the total width. While a single channel gives rise to a series of resonances converging to the relevant ionization threshold, these resonances are generally not resolved in the experimental DR data. Thus, following Mikhailov et al. [20], we average over the resonances to give

$$\langle\sigma\rangle \approx \frac{2\pi^2}{k^2}\left(\frac{\Gamma_a}{\Delta}\right). \tag{9}$$

where Δ is the spacing between levels, i.e., $\sim 2\mathcal{R}/n^{*3}$. Because Γ_a and Δ both scale as $\sim 1/n^{*3}$, the expression in parentheses is approximately independent of n and equal to $4\pi\tilde{D}\omega^2$. As discussed previously [7], this cross section is multiplied by the relative velocity and convolved with the experimental transverse and parallel spreads in the electron velocity to provide the recombination rate.

TABLE I. Jahn-Teller parameters for the $3pE'$ state of H_3 and its isotopomers.

Species	ω^+ (cm^{-1})	$D\omega^a$ (cm^{-1})	$D^{1/2}$	$\tilde{D}^{1/2}$ (cm)^b
H_3	2521.20^c	75.89	0.1735	1.4447×10^{-5}
H_2D	2205.87^d	75.89	0.1855	1.5446×10^{-5}
HD_2	1968.17^d	75.89	0.1964	1.6354×10^{-5}
D_3	1834.67^d	75.89	0.2034	1.6936×10^{-5}

^{a}The value is independent of isotope, and we use the D value of 0.0301 for H_3 $3p$ $^2E'$ from Refs. [16,17].
^{b}This factor represents the scaled value obtained by multiplying $D^{1/2}$ by $n^{*3}/2\mathcal{R}$, with $n^* = 2.634$, the effective principal quantum number of the $3p$ $^2E'$ state.
^{c}The *ab initio* result of Ref. [18].
^{d}The *ab initio* result of Ref. [19].

Figure 2 shows the resulting DR rate coefficient for H_3^+, along with the experimental data of Kreckel et al. [21] between 0.0001 and 0.4 eV. Also shown are the results of the calculation of Fonseca dos Santos et al. [9]. The agreement of the present model with the previous results is good. The present results drop to zero at energies above $\omega_2^+(H_3^+) \sim 0.31$ eV because the $\Delta v_2 = 1$ capture process is no longer possible above the $v_2^+ = 1$ threshold. Above this energy, $\Delta v_2 \geq 2$ processes must be responsible for DR, but according to the vibrational propensity rule, these processes are expected to produce much smaller capture widths. In addition, $\Delta v_1 = 1$ processes are possible up to $\omega_1^+(H_3^+) \sim 0.39$ eV, but these are not considered here. Note that both the experimental and previous theoretical rates show a substantial drop near the $v_2^+ = 1$ threshold, as expected from the propensity rule for vibrational autoionization or capture.

Figure 3 shows our results for the DR rates for the four isotopomers H_3^+, H_2D^+, HD_2^+, and D_3^+, along with the corresponding experimental data [21–23] and previous theoretical results [7–9]. For D_3^+, the 40 meV convolution of Ref. [8] was used because it smooths out resonant structure not observed in the experiment. Overall, the agreement is good for all four isotopomers, although the results for D_2H^+ are a factor of 2–3 below the experimental result [23]. Indeed, the present model predicts a very simple isotope dependence, with decreasing rates for increasing mass, and with the D_3^+ rate lying a factor of $\sim 1/\sqrt{2}$ below the H_3^+ result. This dependence is somewhat obscured because the electron velocity spreads were different in the different measurements. The only other significant discrepancy is the lack of a rapid falloff of the
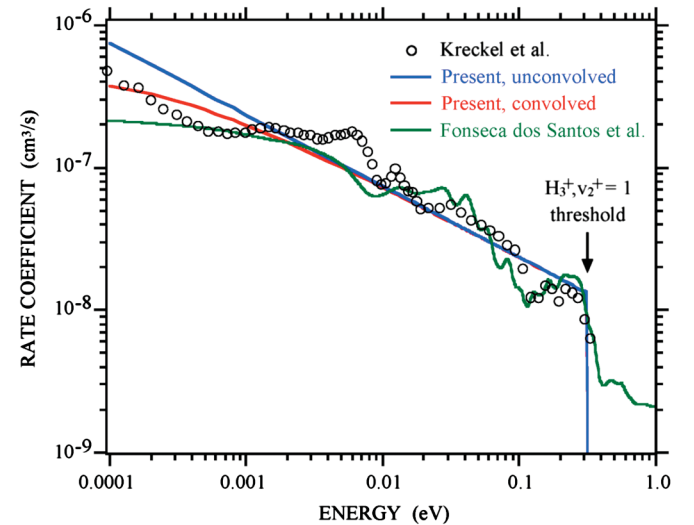

FIG. 2 (color). The DR rate coefficient of H_3^+ as a function of collision energy. Circles: experiment [21] with $\Delta E_\perp = 0.5$ meV and $\Delta E_\parallel = 0.025$ meV; Solid line: present results, unconvolved. Dotted line: present results, convolved with $\Delta E_\perp = 0.5$ meV and $\Delta E_\parallel = 0.025$ meV; Dashed line: theoretical data [9], convolved with $\Delta E_\perp = 2$ meV and $\Delta E_\parallel = 0.1$ meV.
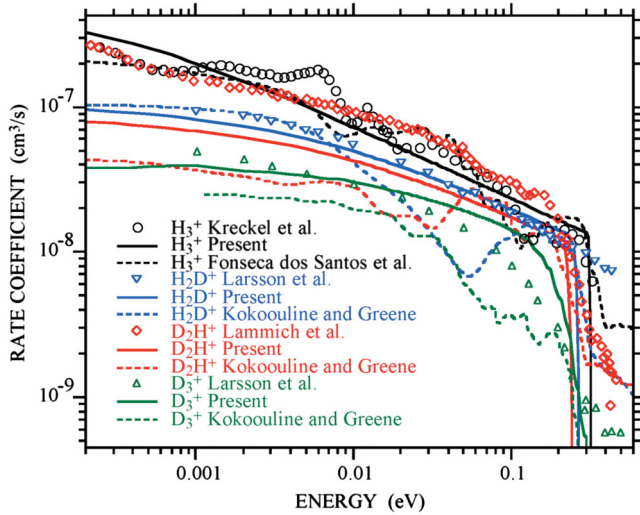
FIG. 3 (color).   The DR rate coefficient of an electron and H_3^+, H_2D^+, D_2H^+, and D_3^+ as a function of collision energy. H_3^+ (black) Circles: experiment [21] with $\Delta E_\perp = 0.5$ meV and $\Delta E_\parallel = 0.025$ meV; Solid line: present results, convolved with $\Delta E_\perp = 0.5$ meV and $\Delta E_\parallel = 0.025$ meV; Dashed line: theoretical results [9] convolved with $\Delta E_\perp = 2$ meV and $\Delta E_\parallel = 0.1$ meV, and with a rotational temperature of 1000 K. H_2D^+ (blue) Inverted triangles: experiment [22]; Solid line: present results, convolved with $\Delta E_\perp = 10$ meV and $\Delta E_\parallel = 0.2$ meV; Dashed line: theoretical results [7] convolved with $\Delta E_\perp = 10$ meV and $\Delta E_\parallel = 0.2$ meV. D_2H^+ (red) Diamonds: experiment [23] with $\Delta E_\perp = 12$ meV and $\Delta E_\parallel = 0.07$ meV; Solid line: present results, convolved with $\Delta E_\perp = 12$ meV and $\Delta E_\parallel = 0.07$ meV; Dashed line: theoretical results [7] convolved with $\Delta E_\perp = 10$ meV and $\Delta E_\parallel = 1$ meV. D_3^+ (green) Triangles: experiment [22]; Solid line: present results, convolved with $\Delta E_\perp = 40$ meV and $\Delta E_\parallel = 6$ meV; Dashed line: theoretical results [8] convolved with $\Delta E_\perp = 40$ meV and $\Delta E_\parallel = 6$ meV.

experimental H_2D^+ rate at energies above the $\nu_2^+ = 1$ threshold [22]. If confirmed by future experiments, this observation would indicate the importance of a second mechanism for DR in this energy region.

In summary, the present model provides an independent, experimentally based determination of the DR of H_3^+ and its isotopomers. The good agreement with existing experimental and theoretical data confirms the conclusion of Refs. [6–9] that the JT interaction in the np Rydberg states drives the electron capture process. The use of high-quality spectroscopic data on low-lying states of H_3 to describe the DR process is central to the present approach, and provides a connection between two very different kinds of experimental data. The model also provides a first-order prediction of the isotopic dependence of the reaction. While high-level calculations [6–9] will always be necessary to account for the details of the experimental data (which are rapidly improving to reveal vibrational, rotational, and even nuclear spin effects, as well as better resolved reso-

nances), the present model may provide a means to assess the role of indirect capture mechanisms in more complicated systems (e.g., H_3O^+ or NH_4^+) without requiring large-scale computation.

*Also at Department of Physics and Astronomy, University College London, London WC1E 6BT, United Kingdom.
[1] T. Oka, in *Dissociative Recombination of Molecular Ions with Electrons* edited by S. L. Guberman (Kluwer Academic/Plenum Publishers, New York, 2003), p. 209.
[2] E. Herbst and W. Klemperer, Astrophys. J. **185**, 505 (1973).
[3] See, for example, *The Molecular Astrophysics of Stars and Galaxies*, edited by T. W. Hartquist and D. A. Williams (Clarendon Press, Oxford, 1998).
[4] M. Larsson and A. E. Orel, *Dissociative Recombination of Molecular Ions* (Cambridge, New York, 2008).
[5] M. Larsson, B. J. McCall, and A. E. Orel, Chem. Phys. Lett. **462**, 145 (2008).
[6] V. Kokoouline, C. H. Greene, and B. D. Esry, Nature (London) **412**, 891 (2001).
[7] V. Kokoouline and C. H. Greene, Phys. Rev. A **72**, 022712 (2005).
[8] V. Kokoouline and C. H. Greene, Phys. Rev. A **68**, 012703 (2003).
[9] S. Fonseca dos Santos, V. Kokoouline, and C. H. Greene, J. Chem. Phys. **127**, 124309 (2007).
[10] G. Herzberg, *Molecular Spectra and Molecular Structure* (Krieger, Malabar, 1991), Vols. I and III.
[11] G. Herzberg, Annu. Rev. Phys. Chem. **38**, 27 (1987).
[12] H. C. Longuet-Higgins, Adv. Spectros. **2**, 429 (1961).
[13] M. V. Berry, Proc. R. Soc. A **392**, 45 (1984).
[14] R. S. Berry, J. Chem. Phys. **45**, 1228 (1966).
[15] G. Herzberg and Ch. Jungen, J. Mol. Spectrosc. **41**, 425 (1972).
[16] G. Herzberg and J. K. G. Watson, Can. J. Phys. **58**, 1250 (1980).
[17] G. Herzberg *et al.*, Can. J. Phys. **59**, 428 (1981).
[18] R. Jaquet *et al.*, J. Chem. Phys. **108**, 2837 (1998).
[19] O. Polyansky and J. Tennyson, J. Chem. Phys. **110**, 5056 (1999).
[20] I. A. Mikhailov *et al.*, Phys. Rev. A **74**, 032707 (2006).
[21] K. Kreckel *et al.*, Phys. Rev. Lett. **95**, 263201 (2005); see also, B. J. McCall *et al.*, Nature (London) **422**, 500 (2003); B. J. McCall *et al.*, Phys. Rev. A **70**, 052716 (2004).
[22] M. Larsson *et al.*, Phys. Rev. Lett. **79**, 395 (1997).
[23] L. Lammich *et al.*, Phys. Rev. Lett. **91**, 143201 (2003).